A Review of Groundwater Chemistry Monitoring Data at Ranger

DA Klessa

Abstract

The chemistry of groundwater at Ranger over the period June 1981–November 2000 was reviewed with particular emphasis on the bore monitoring data which ERA is required to provide under the current General Authorisation. Most of this data is linked to the monitoring of groundwater contamination in the vicinity of the tailings dam. The main purpose of this study was to examine, model and predict the breakthrough of contaminants at bores using available information.

Whilst groundwater at the tertiary bores shows enhanced solute concentrations indicative of mining impact, in all cases the process is in its early stages as shown by the exponential growth form of concentration vs time relationships. Consequently, historical data from observation bores (OB) 11a, 13a, 15 and 16 which are no longer monitored but which show strong evidence of solute breakthrough from the sigmoidal (concentration vs time) function, were used to derive a predictive model based upon a characteristic SO_4:Mg ratio at SO_4 breakthrough. This then allowed the breakthrough time and inferred rate of (conservative) solute movement to be extrapolated from the simultaneous solving of the exponential growth equations.

Rates of conservative solute movement were estimated in the vicinity of the tailings dam to range from 2 to $8*10^{-7}$ ms^{-1} with relatively higher rates found in the regions of known faults. There was no evidence of ^{226}Ra or U breakthrough but at some tertiary bores small increases in activity/concentration were noted and factors influencing the retardation of ^{226}Ra and U are briefly discussed. As expected, there was a consistent lag in the appearance of Mg^{2+} compared to SO_4. Based on normalised exponential growth functions, the mean gradient of Mg was around 70% of SO_4. Near the dam (0.8–0.9 km), SO_4 breakthrough preceeded Mg by about 100–150 days. The order in the degree of retardation of solutes is $^{226}Ra \geq U > Mn \geq Mg > SO_4$.

Recommendations for further studies are given based upon the implications of breakthrough of tailings solutes into the Gulungul Ck catchment and from Pit#1 to the Corridor Ck catchment.

Introduction

The purpose of this report is to review groundwater chemistry data at Ranger collected by ERA and reported regularly to the statutory authorities. In this respect, only groundwater monitoring data required under the current *Ranger General Authorisation (A82/3)*[1] has been reviewed here (Table 1). Except for two dewatering bores (ie MBL and DW3A), the majority of bores are situated in the locale of the tailings dam and are strategically sited with respect to known faults, hydraulic gradient and, hence, vectors for groundwater movement (Fig 1).

Table 1 List of current designated bores

Primary	Secondary	Tertiary
OB 1A	OB 21A	OB 2A
OB 7A	OB 23	OB 4A
OB 17A	OB 28	OB 6A
OB 19A	OB 43	OB 10A
OB 20		OB 13A
OB 24		OB 29
OB 30		OB 44
OB 41		RN 23552
OB 42A		79/2
RN 23551		

With tailings a potentially significant source term for groundwater contamination, surveillance of bores provides early warning of solute movement as well as quantifying effects on groundwater composition in zones known to be impacted. Consequently, designated bores have been categorised as follows under the *Ranger General Authorisation*:

Primary sites	Bores just ahead and downgradient of the seepage front.
Secondary sites	Bores well ahead of the seepage front.
Tertiary sites	Bores behind the seepage front.

The most useful water quality indicator of groundwater contamination by mining at Ranger, particularly the dispersion of solutes from the tailings dam, is the sulphate ion or as a surrogate, electrical conductivity. The principal cation to sulphate in tailings water, magnesium, is a less useful early warning indicator because of attenuation by negatively charged mineral surfaces. The capacity of the native rock to sorb magnesium and other metals to hamper breakthrough is a function of a number of physical and chemical factors including permeability (ie contact time), local geology/mineralogy and the extent of the weathered zone (ie the presence of secondary clay minerals and sesquioxides), speciation of the contaminants and the proximity of the bore to source terms. However, the risk of heavy metal movement (with the possible exception of manganese) and that of radionuclides is considered low because of the propensity of adsorbing surfaces to attenuate cations and retard movement (Duerden et al 1992).

---

[1] stipulated as 'designated bores' under Annex A.1

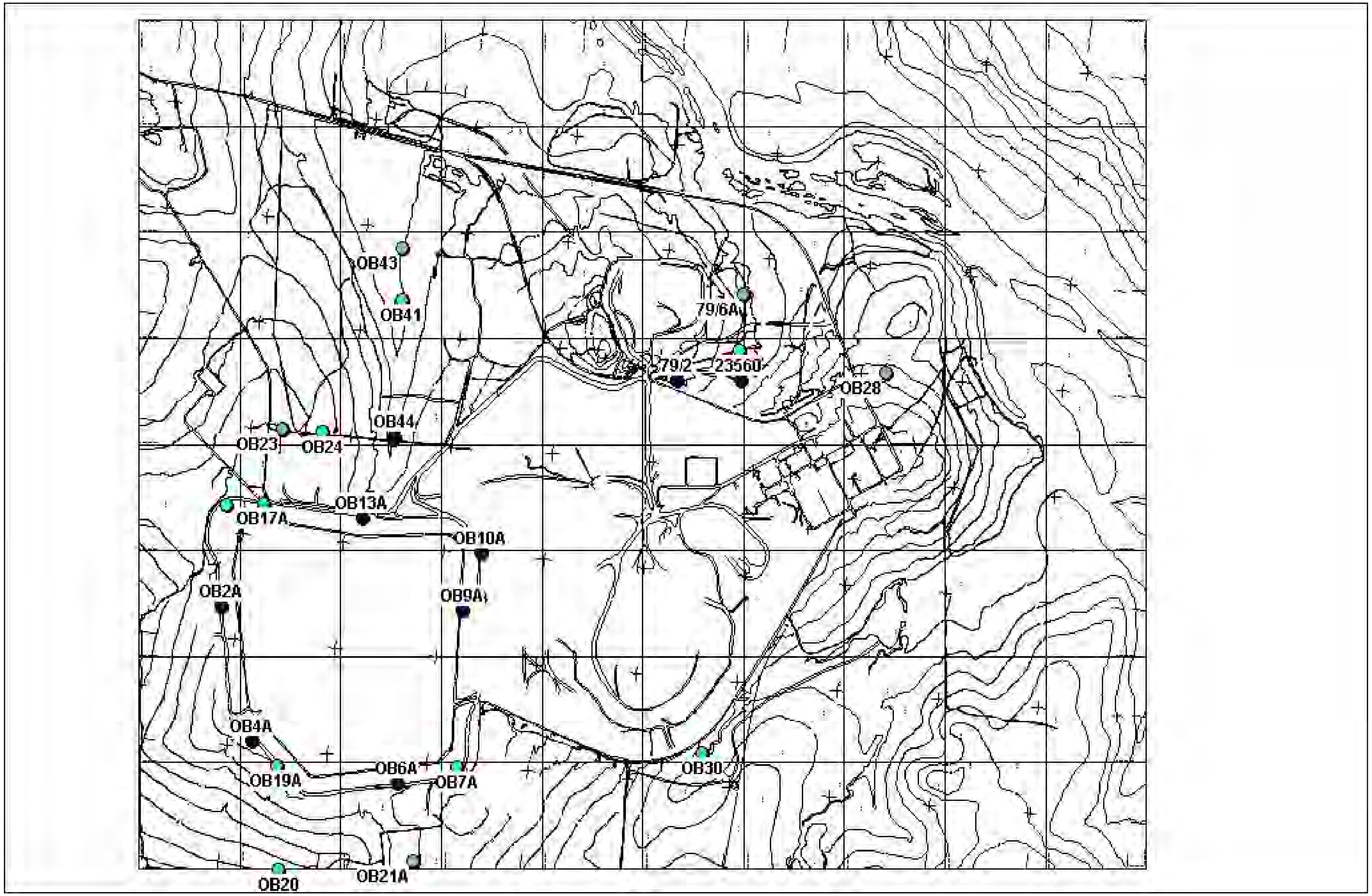

Fig 1 Location of primary (light blue), secondary (blue) and tertiary (black) bores at Ranger

Regional Hydrogeology

A review of studies of the regional hydrogeology of the Ranger mine site and the formulation of a conceptual model has recently been undertaken by Salama & Foley (1997). The following provides a summary of this study as it relates to the current level of understanding of groundwater flow especially in the vicinity of the tailings dam.

Aquifers

Rather than base a classification of aquifers on a a simple shallow/deep mode of occurrence or on a non-carbonate/carbonate lithology as has previously been suggested, Salama & Foley (1997) have proposed a system which recognises zonal influences and host lithologies. Three classes of aquifers are suggested namely *alluvial* (ie shallow), *weathered rock* (intermediate in depth) and *fractured rock* (deep). In addition, local lithology is taken into account as a descriptor which recognises influences on chemistry and hydrology. The lithology classes are *superficial deposits and alluvium(SD&A)*; *weathered Lower Mine Sequence(WLMS)* ; *weathered Upper Mine Sequence (WUMS)*; *weathered Hanging Wall Sequence (WHWS)*; *weathered Nanambu Complex (WNC)*; *fractured (F)LMS*; *FUMS*; *FHWS* and *FNC*. In the vicinity of the tailings dam, bores intercept *SD&A*, *WNC* and *FNC*. According to Salama & Foley (1997), these aquifers have the following chemical characteristics listed in the order– cation facies, anion facies, pH and EC (µScm^{-1}):

Superficial deposits and alluvium	Ca–Na, HCO_3–Cl, 5.5, <50
Weathered Nanambu complex	Na–Ca–Mg, HCO_3–Cl, 6.0–6.5, <200
Fractured Nanambu complex	Ca-Na, HCO_3 and HCO_3–Cl-SO_4, 6.6–7.1, 180–310

In general, transmissivities vary within any particular aquifer by at least an order of magnitude. These are listed along with storage coefficients in Table 2 (Verma & Salama 1986; as given in Salama& Foley 1997).

Table 2 Transmissivity and storage coefficients of aquifers in the Ranger mine area

Aquifer	Transmissivity (m^{2}d^{-1})	Storage coefficient
Carbonate	83.0-470.0	1.0^{-1} – 7.8^{-3}
Shallow	4.0–101.6	2.4^{-3} – 9.3^{-3}
Weathered	7.7–175.0	1.3^{-3} – 6.9^{-4}
Fractured	20.0–229.0	2.8^{-4} – 5.0^{-4}
Deep	15.0–369.0	1.5^{-4} – 2.4^{-4}

There is some connectivity between the *fractured* and *weathered* aquifers via faults, jounts and dykes (Salama & Foley 1997). To the north of the tailings dam, the alluvium of Coonjimba Creek expresses water from these deeper aquifers.

Faults and geology of the tailings dam area

The main faults which are known or are inferred in the locale of the tailings dam are shown in Fig 2. The features of these faults are summarised in Table 3 (adapted from Salama & Foley 1997). In reviewing geological studies of the tailings dam area, Salama & Foley (1997) note the predominance of the Nanambu Complex, the major part (75%) of which is augen and

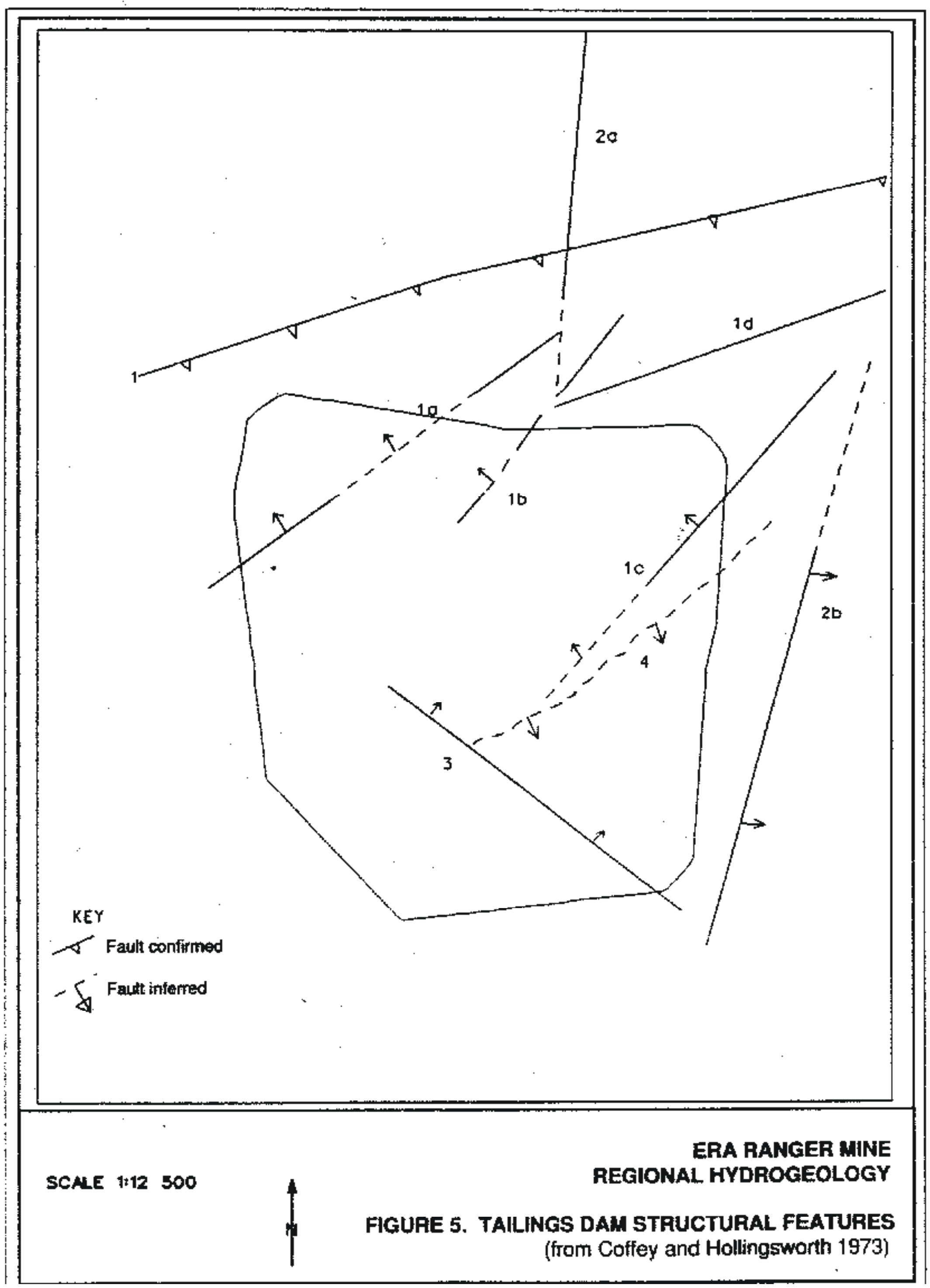

Fig 2 Faults in the vicinity of the Ranger tailings dam (taken from Salama & Foley 1997)

Table 3 Features of the main faults in the environs of the Ranger tailings dam

Identifier	**Location**	**Type**	**Intrusion**	**Fractured**	**Trend**	**Dip**	**Fracture Zone (m)**	**Faults Zone (m)**	**$F_a^\dagger$**	**Permeability**
1	north of dam	thrust	yes	yes	77º of N	40º S	>50	~50	~1	conduit
1a	north wall	secondary thrust	yes	yes	50º of N	60º NW	20–50	~20	~1	conduit
1b	north & west walls	secondary thrust	yes	yes	40º of N	60º NW	20–50	~20	~1	conduit
1c	east wall	secondary thrust	yes	yes	40º of N	60º NW	0–20	~5	~1	conduit
1d	north of dam	secondary thrust	yes	yes	80º of N	60º NW	3–5	30–50	~0.1	combined barrier/conduit
2a	north of dam	normal	yes	yes	5º of N	40º E	10–20	30–60	~0.3	combined barrier/conduit
2b	east of dam	normal	yes	no	15º of N	40º E	9	20–40	~0.25–0.45	combined barrier/conduit
3	SE corner of dam	normal	yes	no	128º of N	60º NW	2?	50–150	0.01–0.04	barrier
4	east wall	thrust	no	yes	50º of N	shallow	2	6–9	0.2–0.3	combined barrier/conduit

† where F_a = damage zone width/total fault zone width

granitic gneiss with minor schists and pegmatite. Variations include migmatitic gneiss (north-west corner of the dam), interlayered schist (south-east), quartz feldspar pegmatite (south-east with NW trend), amphibolite (central north wall with NW trend), and quartz/mica felspar schist and quartz biotite schist (north-east and north-west to south-west dam wall, and north of the dam). The higher permeability of the '1' faults has been confirmed by field pumping tests (Salama & Foley 1997) although the west wall region shows low permeability. The area around the north wall, particularly between Faults 1a and 1b shows high permeability which extends through to 2a by intersection (Salama & Foley 1997). Transmissivities in the vicinity of the north wall are around 10–76 m^2d^{-1}, at the west wall 3–10 m^2d^{-1}, to the west of Fault 2a about 8–16 m^2d^{-1}, and to the east of Fault 2a 6–8 m^2d^{-1} (Salama & Foley 1997).

Bores

Slotted depths of the bores sunk in the locale of the tailings dam are given in Table 4 and mainly intercept *WNC* and *FNC* (see p 5).

Table 4 Slotted depths for the Ranger observation bores

Bore	Bore Depth (m)	Slotted depth (m)
OB1A	31.0	16.0 - 31.0
OB2A	30.0	15.0 - 30.0
OB4A	37.0	22.0 - 37.0
OB6A	26.0	14.0 - 26.0
OB7A	30.0	15.0 - 30.0
OB9A	30.0	12.0 - 30.0
OB10A	30.0	12.0 - 30.0
OB13A	30.0	10.0 - 30.0
OB17A	41.0	23.30 - 41.0
OB19A	51.20	33.0 - 51.20
OB20	36.18	21.0 - 36.18
OB21A	43.0	31.0 - 43.0
OB23	51.30	36.20 - 51.30
OB24	36.50	21.50 - 36.50
OB28	46.40	31.0 - 46.40
OB29	50.40	35.0 - 50.40
OB30	47.50	20.0 - 35.0
OB41	25.0	16.45 - 24.65
OB42A	N/A	N/A
OB43	22.0	15.70 - 21.70
OB44	16.10	11.10 - 16.10
79/2	60.0	11.0 - 15.0

Results and Discussion

Primary sites

Data for the primary bores are summarised in Figs 2-4 and Tables 8–12 (Appendix). Given their classification as primary bores, they are not, for the most part, impacted by mine influences. However, there are a few exceptions these being;

OB 7A	SO_4 and Mg
OB 19A	SO_4
OB 30	SO_4 and Mg

The interpretation of the trends shown by these bores is discussed elsewhere (p 22 and Table 5).

In general, the chemistry of primary bore waters are relatively concordant in time and space with the greatest variability between and within bore waters shown by Mn and U (Fig 4). In the case of the former, differences in mineral facies combined with seasonal redox effects, exacerbate these differences. For U, some poor data points confound and exaggerate variability. However, none of the bores show upward trends in Mn, U or ^{226}Ra.

Secondary sites

By definition, secondary bores lie well ahead of a moving solute front. This is confirmed by the data (Fig 4) which provides no evidence of impact. Box plots are given in Fig 5 and a statistical summary is provided in Table (Appendix). In OB21, there is the suggestion that an upward trend in Mn has been taking place over the last 3 years in the absence of any other major change in chemistry. The reason for this is unclear but may be linked to the succession of wetter than normal years which has increased ground water height leading to Mn reduction (in the shallow aquifer) and its migration into the *fractured* aquifer.

Tertiary sites

Concentrations of Mg,Mn and SO_4 are graphed over time in Figs 7 & 8 and data for pH, EC, Mn, Mg, SO_4 and U are summarised in Fig 9 and Table (Appendix).

Hydrodynamic modelling was undertaken using Mg, Mn and SO_4 data which were augmented by data from OB11a, OB15 and OB16 whose monitoring no longer forms part of the Authority to Operate. In the fullness of time, hydrodynamic dispersion of conservative solutes from a tailings dam source is expected to yield sigmoidal relationships between concentration and time. Modification of these relationships, particularly to the rate of breakthrough, will occur if chemical interaction between the host rock and solute occurs (ie adsorption) or if holdback from poor interconnectivity of flow paths (ie zones of lower hydraulic conductivity) is seen. The degree of holdback from chemical effects is entirely dependent on speciation but for the indicators which are examined here the order is expected to be $Mn^{2+} \geq Mg^{2+} > SO_4^{2-}$. However, holdback from adsorption will tend to be a first contact phenemonon. As the time of contact between solute and surfaces increases, saturation of adsorption sites will negate further retention.

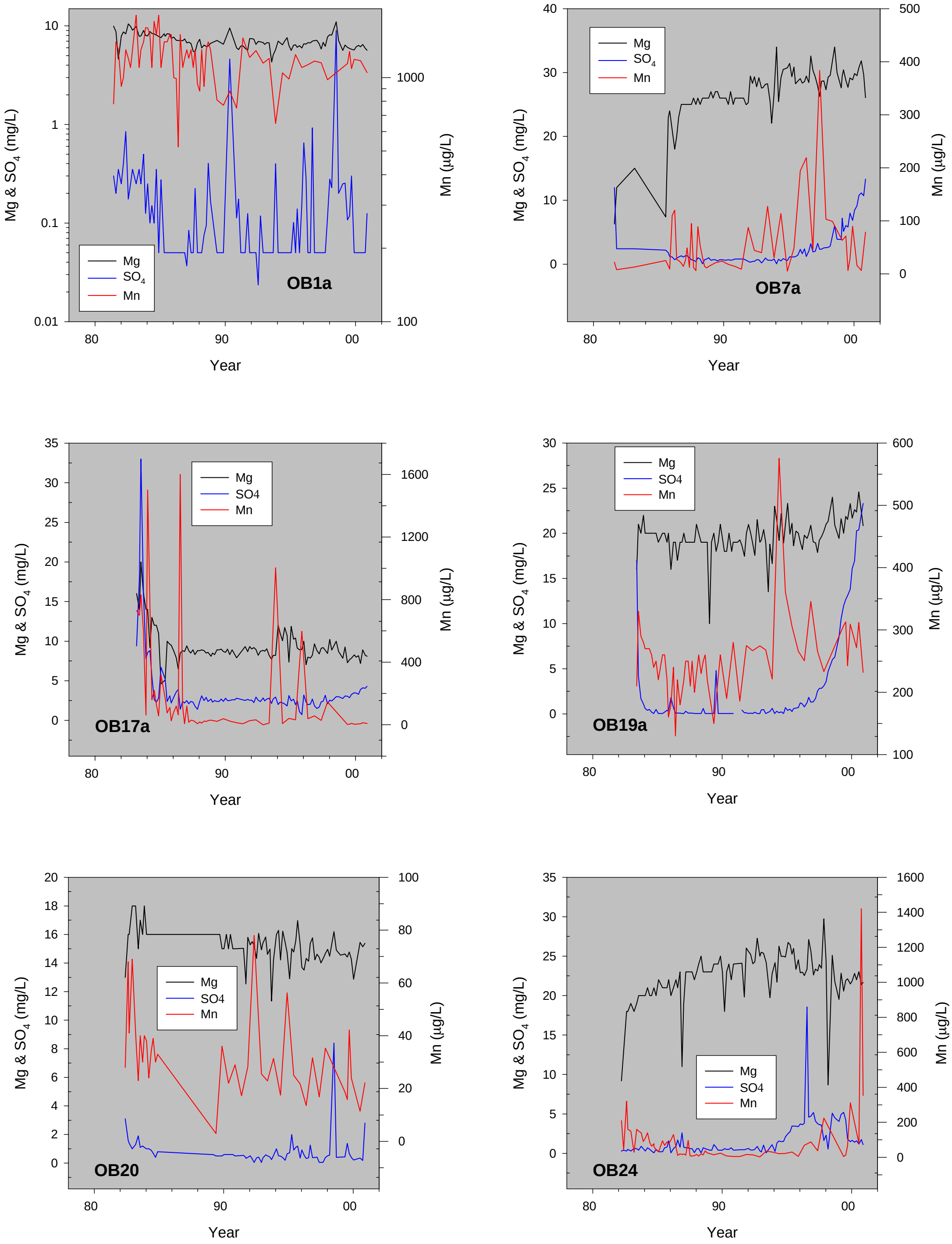

Fig 2 Dissolved Mg^{2+}, SO_4^{2-} and Mn^{2+} in groundwater at OB 1A, 7A, 17A, 19A, 20 and 24

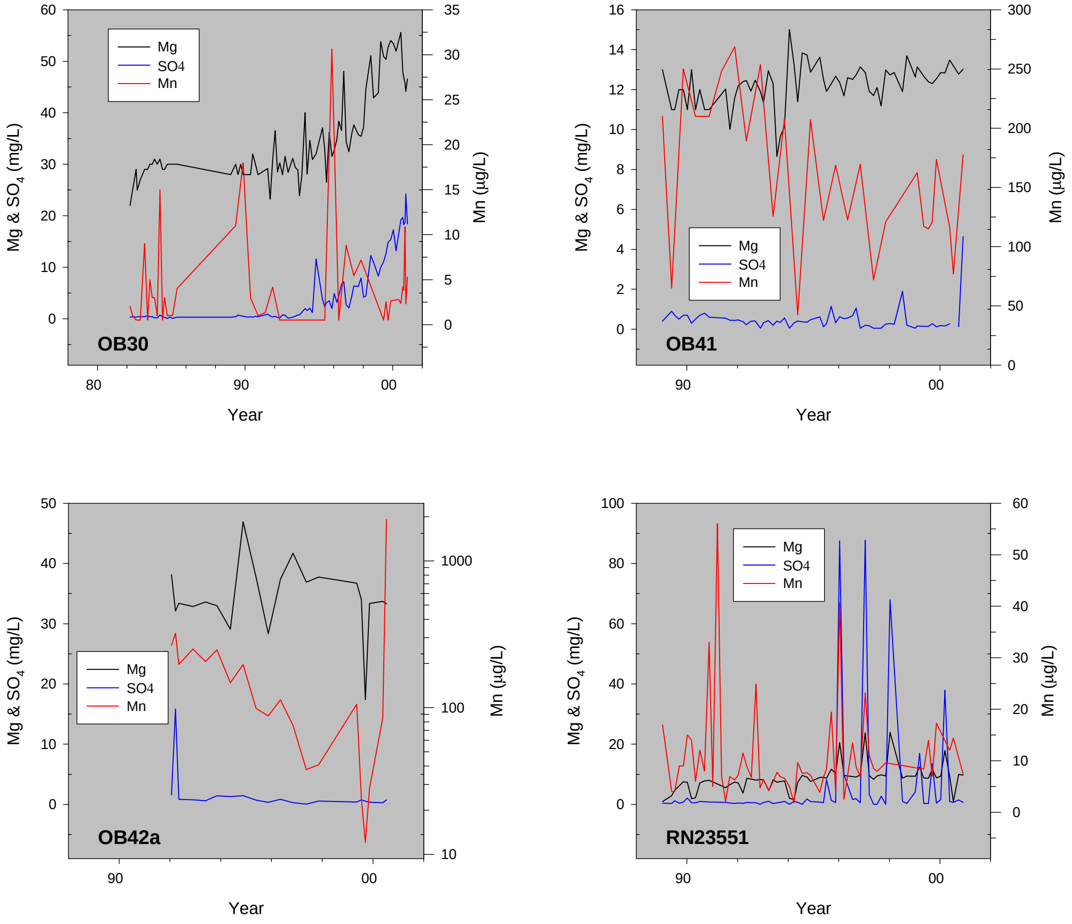

Fig 3 Dissolved Mg^{2+}, SO_4^{2-} and Mn^{2+} in groundwater at OB 30, 41, 42A and RN 23551

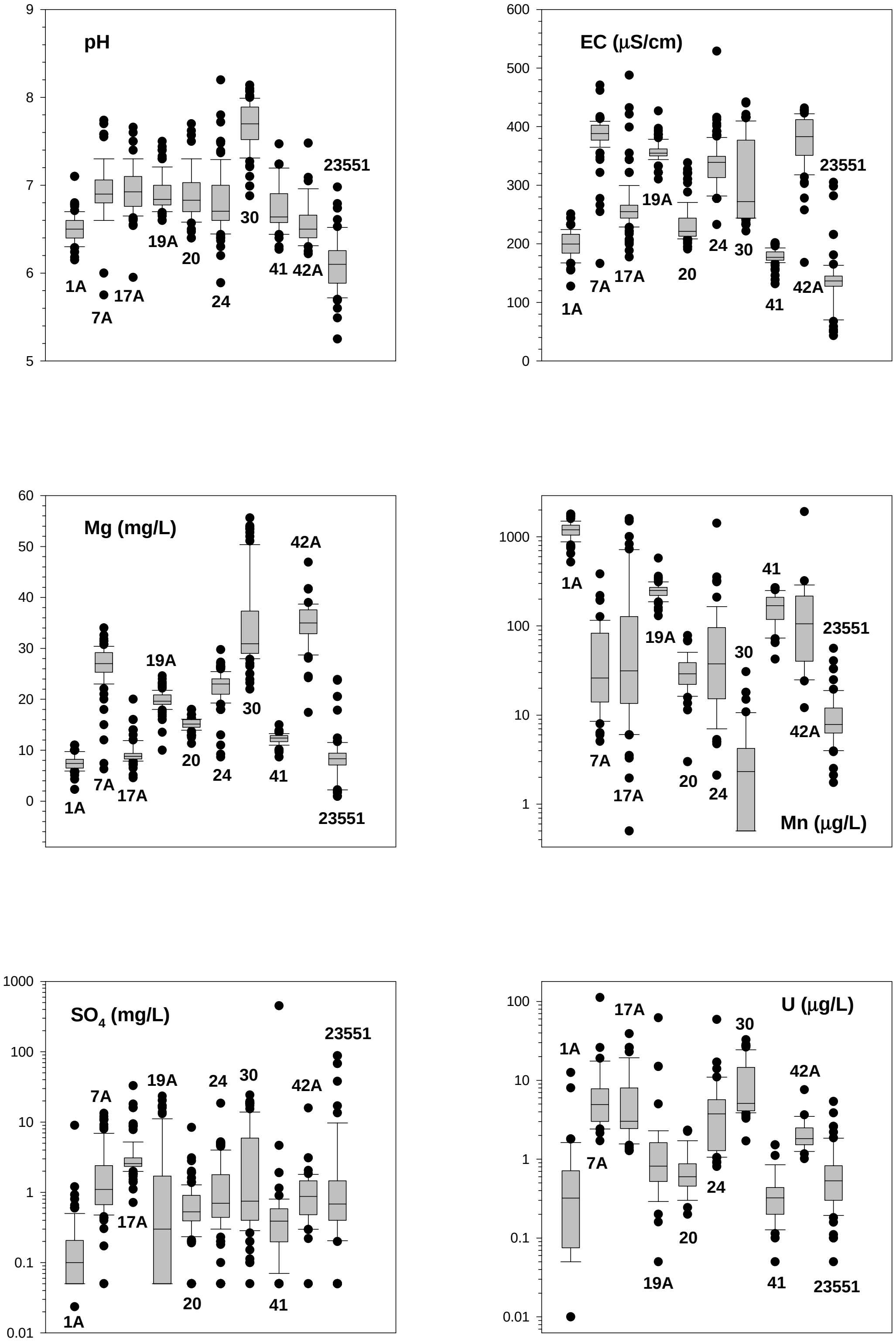

Fig 4 Boxplots of pH and EC and dissolved Mg, Mn, SO_4 and U in the groundwater of primary bores

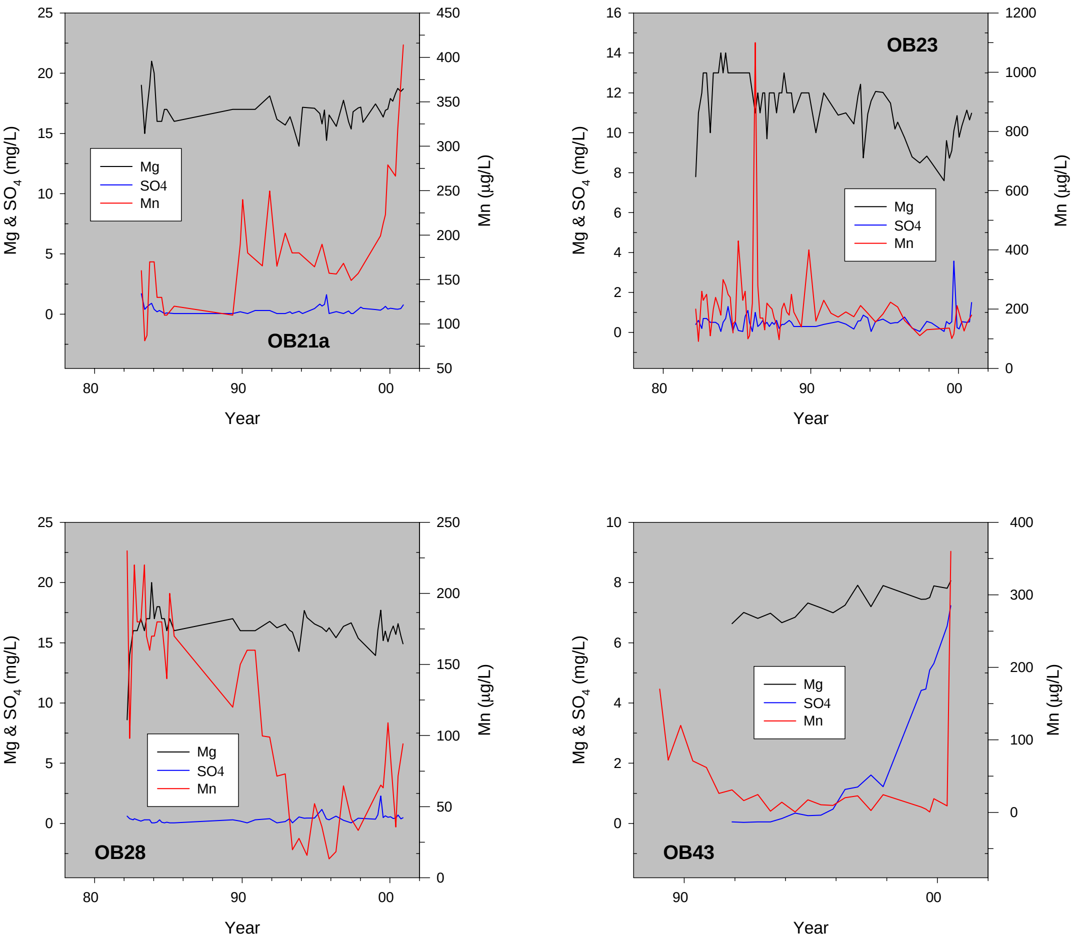

Fig 5 Dissolved Mg^{2+}, SO_4^{2-} and Mn^{2+} in groundwater at OB 21A, 23, 28 and 43

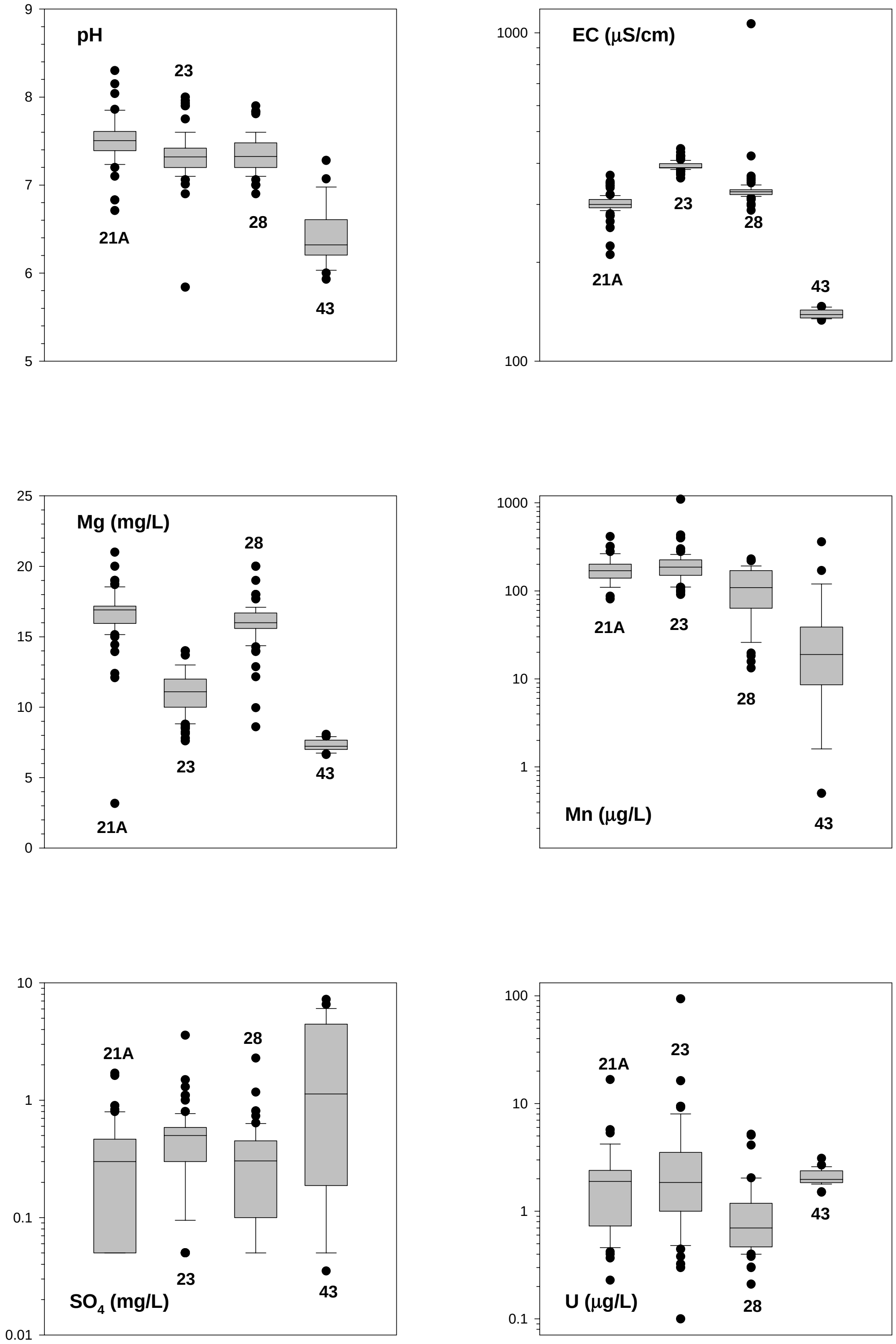

Fig 6 Boxplots of pH and EC and dissolved Mg, Mn, SO_4 and U in the groundwater of secondary bores

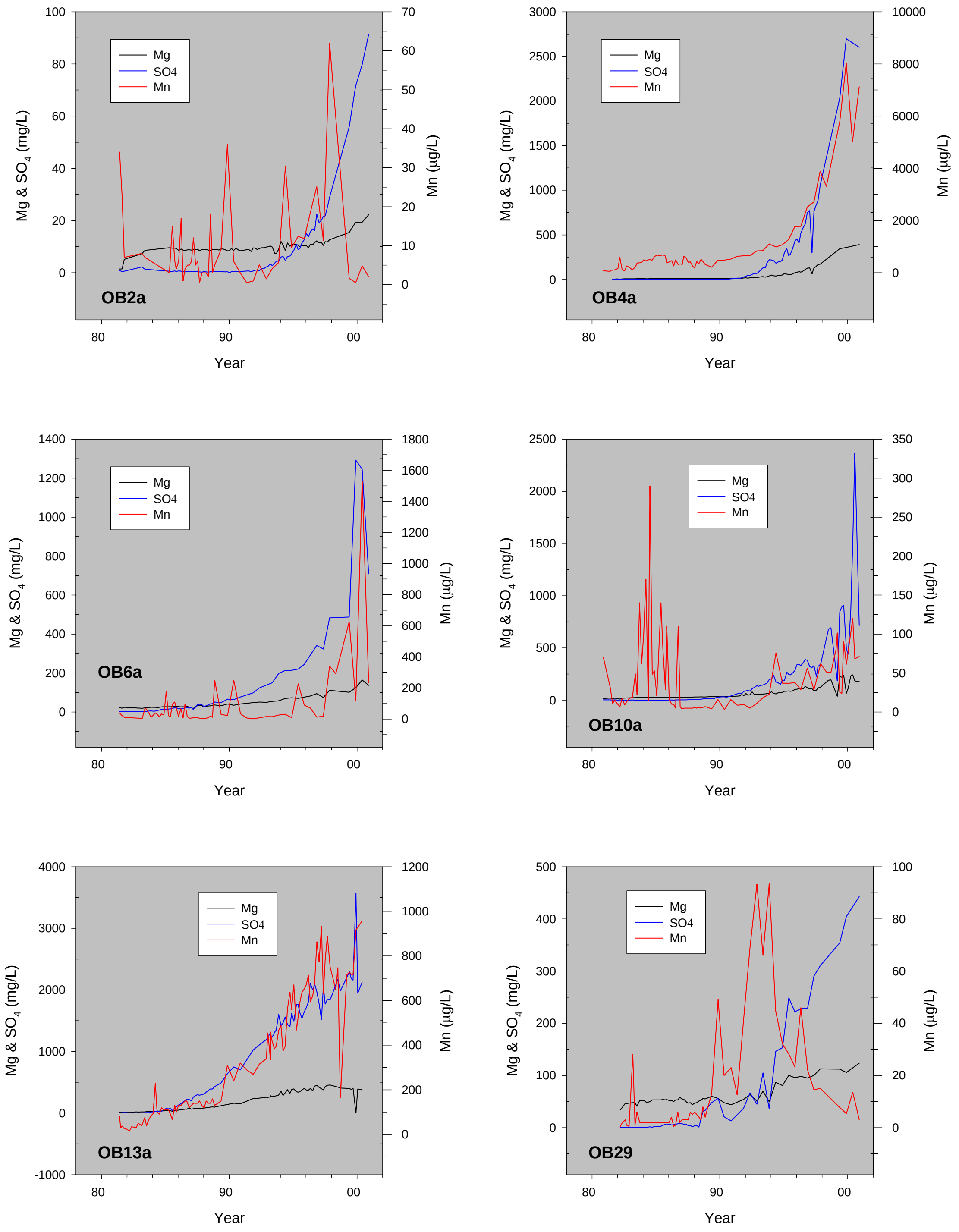

Fig 7 Dissolved Mg^{2+}, SO_4^{2-} and Mn^{2+} in groundwater at OB 2A, 4A, 6A, 10A, 13A and 29

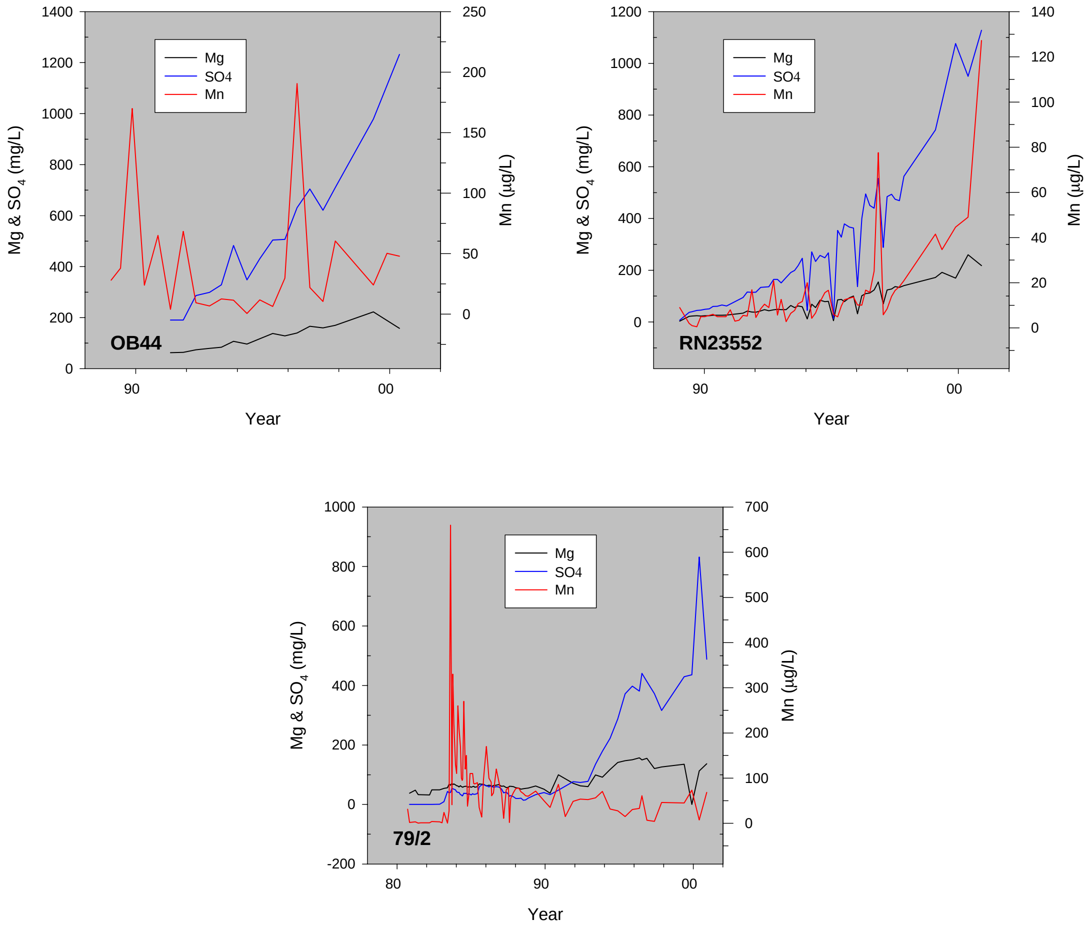

Fig 8 Dissolved Mg^{2+}, SO_4^{2-} and Mn^{2+} in groundwater at OB 44, RN 23552 and 79/2

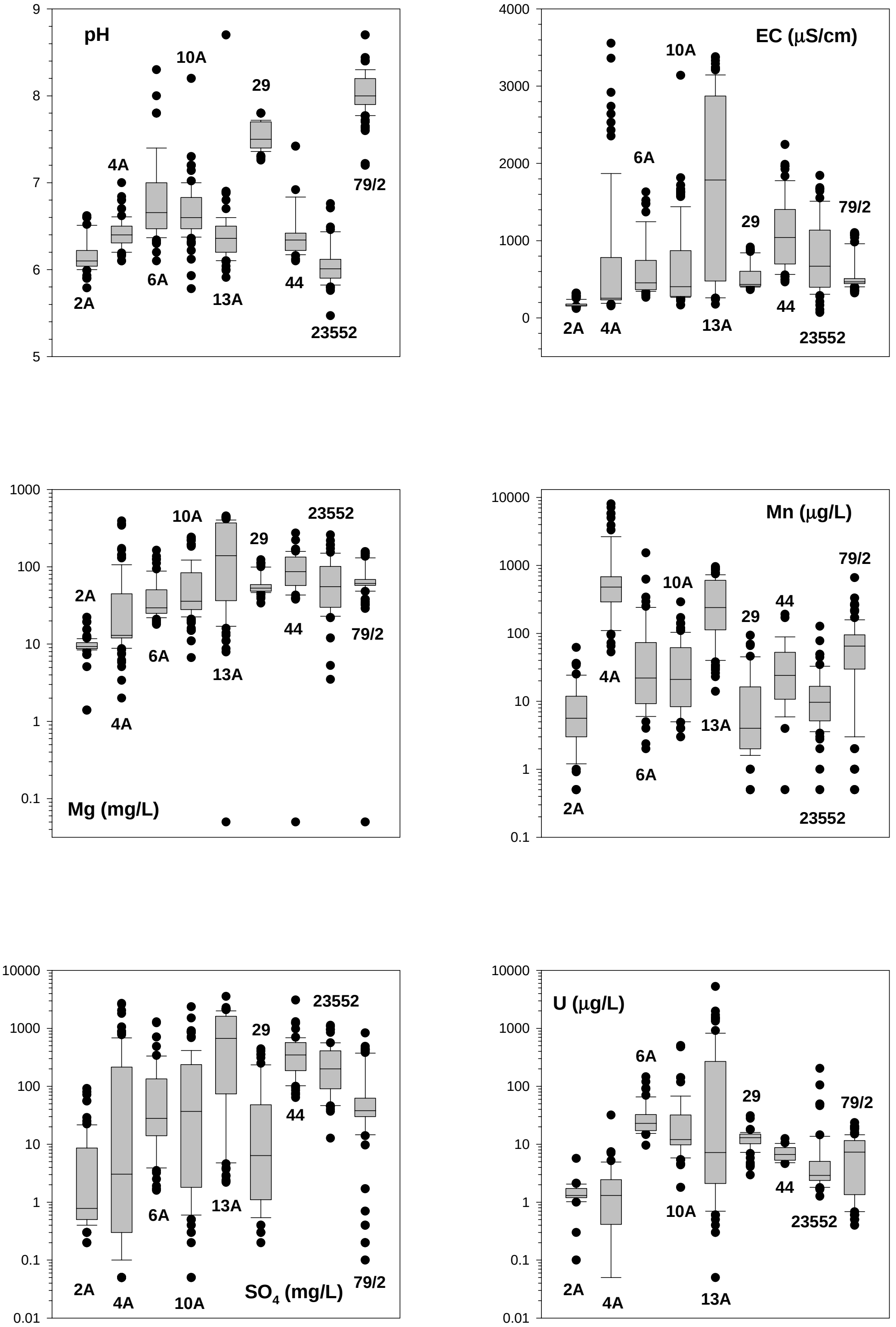

Fig 9 Boxplots of pH and EC and dissolved Mg, Mn, SO_4 and U in the groundwater of tertiary bores

The form of the sigmoid used in modelling was a 4 variable exponential *viz*

$$y = y_0 + \frac{a}{1 + \exp^{-\left\{\frac{t - t_0}{b}\right\}}} \quad \ldots\ldots\ldots\ldots\ldots\ldots 1.$$

where

y = concentration (mg/L or µg/L)

y_0 = lower asymptote

a = upper asymptote

t_0 = point of inflection

t = time (day)

b = gradient at point of inflection

In most cases, however, a sigmoid was not shown and a 3 variable exponential growth function of the following form was fitted to the data *viz*

$$y = y_0 + a \exp^{bt} \quad \ldots\ldots\ldots\ldots\ldots\ldots 2.$$

Examples of the two forms of fitted functions are given in Fig 10.

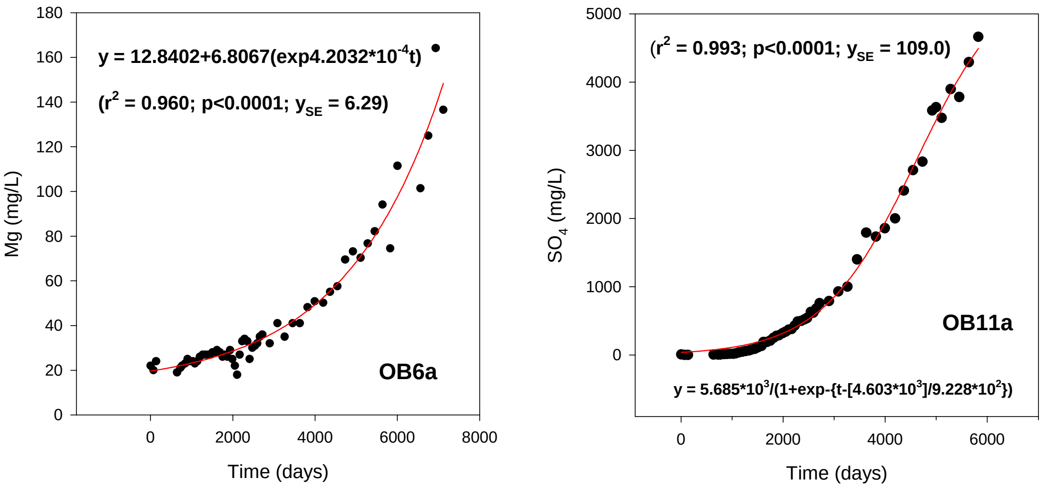

Fig 10 Examples of fitted exponential growth (left) and sigmoidal (right) functions to bore water data

Results are summarised in Tables 5 and 6 respectively for the exponential growth and sigmoidal function fitting respectively. In all cases, 1 June 1981 was taken as day 1 for modelling purposes which coincides with the time when the tailings dam was first used as a repository. For RN23552, monitoring started in 1989 and there was no evidence of a lag phase to an increase in concentration of dissolved species. Consequently a 2 variable growth curve was fitted (see Table 5 note). Similarly, for OB11a and OB16 data better fits were obtained with a 3 parameter sigmoid (Table 6).

Table 5 Fitted values, goodness of fit and standard errors for two and three parameter exponential growth functions

		Parameter					Standard errors			
Bore	**Species**	**y_0**	**a**	**b**	**Corrected r^2**	**Significance**	**y**	**y_0**	**a**	**b**
OB2a	Mg	8.852	$3.846*10^{-3}$	$1.147*10^{-3}$	0.914	<0.0001	0.760	0.1179	$1.805*10^{-3}$	$6.786*10^{-5}$
	SO_4	0.05†	$3.06*10^{-2}$	$1.134*10^{-3}$	0.991	<0.0001	1.582	0.254	$4.264*10^{-3}$	$2.029*10^{-5}$
OB4a	Mg	4.474	0.456	$9.682*10^{-4}$	0.957	<0.0001	14.17	2.168	$9.75*10^{-2}$	$3.171*10^{-5}$
	Mn	247.5	21.977	$8.182*10^{-4}$	0.929	<0.0001	422.3	74.63	8.979	$5.981*10^{-5}$
	SO_4	0.05†	1.806	$1.035*10^{-3}$	0.935	<0.0001	122.5	17.57	0.556	$4.518*10^{-5}$
OB6a	Mg	12.84	6.807	$4.203*10^{-4}$	0.960	<0.0001	6.29	3.00	1.632	$3.324*10^{-3}$
	SO_4	0.05†	5.94	$7.326*10^{-4}$	0.859	<0.0001	95.95	2.07	3.533	$8.723*10^{-5}$
OB10a	Mg	11.76	5.83	$4.955*10^{-4}$	0.806	<0.0001	23.89	6.76	2.571	$6.216*10^{-5}$
	SO_4	4.25	1.861	$9.168*10^{-4}$	0.740	<0.0001	166.9	25.11	1.385	$1.124*10^{-4}$
OB15	Mg	–	8.736	$7.194*10^{-4}$	0.988	<0.0001	14.84	–	0.692	$1.521*10^{-5}$
	Mn	–	86.23	$4.411*10^{-4}$	0.799	<0.0001	131.8	–	13.74	$3.374*10^{-5}$
OB29	Mg	37.71	6.436	$3.740*10^{-4}$	0.861	<0.0001	7.74	4.58	2.864	$6.136*10^{-4}$
	SO_4	0.05†	6.809	$6.066*10^{-4}$	0.929	<0.0001	28.10	7.29	2.226	$4.739*10^{-5}$
OB44	Mg	–	15.47	$3.937*10^{-4}$	0.902	<0.0001	15.14	–	1.475	$1.708*10^{-5}$
	SO_4	-	3.013	$5.316*10^{-4}$	0.944	<0.0001	62.40	–	3.013	$1.740*10^{-5}$
RN23552‡	Mg	–	4.234	$5.694*10^{-4}$	0.876	<0.0001	19.35	–	0.771	$2.949*10^{-5}$
	SO_4	–	8.159	$7.002*10^{-4}$	0.926	<0.0001	70.34	–	1.444	$2.836*10^{-5}$
OB7a	SO_4	0.776	$2.190*10^{-4}$	$1.536*10^{-3}$	0.949	<0.0001	0.624	0.086	$1.194*10^{-4}$	$7.862*10^{-5}$
OB19a	SO_4	0.456	$5.743*10^{-5}$	$1.828*10^{-3}$	0.858	<0.0001	1.900	0.230	$5.015*10^{-3}$	$1.514*10^{-4}$
OB30	Mg	0.272	0.276	$6.367*10^{-4}$	0.776	<0.0001	4.010	1.032	0.184	$9.346*10^{-5}$
	SO_4	0.120	$1.880*10^{-2}$	$9.819*10^{-4}$	0.927	<0.0001	1.587	0.273	$8.721*10^{-3}$	$6.584*10^{-5}$

†Forced y_0; ‡Two parameter exponential growth function fitted of form y = aexpb

Table 6 Fitted values, goodness of fit and standard errors for three and four parameter sigmoid functions

		Parameter						**Standard error**				
Bore	**Species**	**y_0**	**a**	**b**	**t_0**	**Corrected r^2**	**Significance**	**y**	**y_0**	**a**	**b**	**t_0**
OB11a‡	Mg	–	$1.192*10^3$	$9.708*10^2$	$4.702*10^3$	0.997	<0.0001	14.47	–	38.70	22.40	73.30
	SO_4	–	$5.685*10^3$	$9.228*10^2$	$4.603*10^3$	0.993	<0.0001	109.0	–	249.7	34.29	97.80
OB13a	Mg	19.26	$3.826*10^2$	$7.305*10^2$	$3.682*10^3$	0.912	<0.0001	47.37	12.22	23.11	111.3	131.1
	Mn	–	$9.451*10^2$	$1.342*10^3$	$4.555*10^3$	0.893	<0.0001	92.34	–	91.10	151.9	326.0
	SO_4†	2.50	$2.429*10^3$	$1.001*10^3$	$4.289*10^3$	0.953	<0.0001	176.6	56.11	164.0	123.1	124.7
OB15	SO_4	–	$3.017*10^3$	$7.911*10^2$	$4.973*10^3$	0.980	<0.0001	86.75	–	277.1	57.98	166.3
OB16‡	Mg	–	$6.751*10^2$	$1.122*10^3$	$4.163*10^3$	0.984	<0.0001	19.90	–	36.23	54.79	148.9
	SO_4	–	$2.772*10^3$	$8.897*10^2$	$3.901*10^3$	0.988	<0.0001	81.23	–	93.24	37.69	84.94

†Forced y_0; ‡No minimum asymptote ie fitted equation identical to equation 1 but without y_0 term.

There is a consistent lag in the appearance of Mg^{2+} compared SO_4^{2-} at the bores (Tables 5 & 6) which is expected. For example using the gradient of the normalised exponential growth functions, Mg gradients are between 54–94% of SO_4 (mean = 70%). Similarly, using the sigmoid functions (OB11a and OB16), breakthrough times for SO_4 preceed Mg by about 100–150 days near to the dam (~0.8–0.9 km). Based on sulphate breakthrough times and distances of the bores from the tailings dam inner wall, average rates of solute movement are $2.39*10^{-7}$ (OB11a), $2.27*10^{-7}$ (OB13a) and $2.82*10^{-7}$ (OB16) ms^{-1}. These estimates are in good agreement with estimates of the permeability of the fault zones of 10^{-6}–10^{-7} ms^{-1} by Coffey & Hollingsworth (1976) cited in Salama &Foley (1997).

The exponential growth curves were used to further model expected breakthrough times (in the absence of a point of inflection). Examination of the breakthrough of sulphate (from Table 6 data) showed that the SO_4:Mg ratio (mass/unit volume) was 5.02 (OB11a) , 4.83 (OB15) and 4.65 (OB16). Taking a mean ratio of 4.8 as the signature of SO_4 breakthrough, it is then possible to estimate the point in time from the exponential growth curves at which this condition is satisfied ie

$$\frac{[SO_4]_{pred}}{[Mg]_{pred}} = 4.8$$

An example of the model output is given in Fig 11. In reality, a peak in the ratio would be expected which would then decline to reach quasi steady state. Predictions are summarised in Table 7.

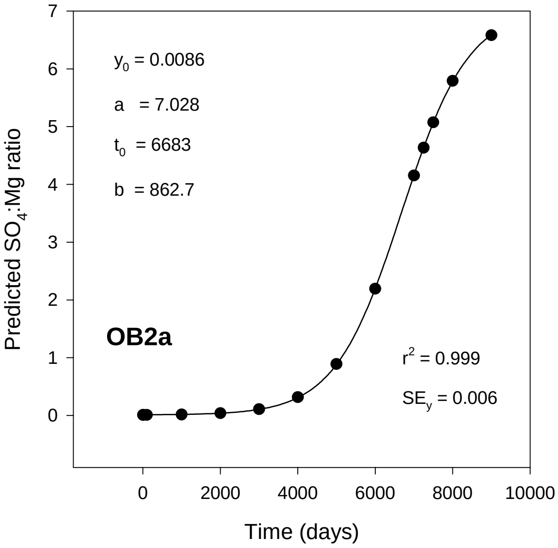

Fig 11 Derived SO_4:Mg ratios over time from the exponential growth functions of SO_4 and Mg at OB2a. Data has been graphed as a 4 variable sigmoid (see equation 1 in the text)

Modelling revealed permeabilities in the range $1.27–7.90*10^{-7}$ ms^{-1} (Table 7) which is consistent with other estimates of movement rates in schist (Salama & Foley 1997). There was very good agreement between breakthrough times for OB44 and RN23552 which showed the fastest solute front arrival times in keeping with the higher permeability of rock in the vicinity of the S–N Fault 2a (Figure 2). The lowest permeabilities were shown in E–W (OB2a), W–E (OB10a) and N–S (OB6a) directions from the tailings dam. Intermediate values

Table 7 Predicted breakthrough times and inferred rates of conservative solute movement at the tertiary bores OB2a, 4a, 6a, 10a, 44 and RN23552 and at the primary bore OB30

Bore	**Form of equation**	**y_0**	**a**	**b**	**t_0**	**corrected r^2**	**Breakthrough (d)**	**Inferred permeability (ms^{-1})**
OB2a	4 parameter sigmoid	$8.6*10^{-3}$	7.028	$8.627*10^{2}$	$6.684*10^{3}$	0.999	7339	$1.27*10^{-7}$
OB4a	3 parameter sigmoid	–	6.918	$1.387*10^{3}$	$3.437*10^{3}$	0.994	4573	$2.46*10^{-7}$
OB6a	2 parameter exp growth	–	0.5498	$3.612*10^{-4}$	–	0.998	5999	$1.57*10^{-7}$
OB10a	2 parameter exp growth	–	0.2579	$4.429*10^{-4}$	–	1	6601	$1.62*10^{-7}$
OB44	2 parameter exp growth	–	1.833	$1.379*10^{-4}$	–	1	6981	$7.90*10^{-7}$
RN23552	2 parameter exp growth	–	1.927	$1.308*10^{-4}$	–	1	6977	$7.71*10^{-7}$
OB30	*3 parameter exp growth*	*0.1124*	*$5.513*10^{-2}$*	*$3.596*10^{-4}$*	–	*0.999*	*12355*	*$2.87*10^{-7}$*

of 2.15, 2.29 and 2.67*10^{-7} ms^{-1} were obtained respectively at OB15, OB11a and OB16 near the north wall of the tailings dam. On the presumption that a similar SO_4:Mg ratio signature might also typify breakthrough at OB30, it was predicted that this would take place in March 2015. However, it is important to note that the increase in dissolved salts at OB30 derives from the effects of weathering of rock from the mining of Pit #1 and not from tailings. Nevertheless, the results suggest that breakthrough of conservative salts in tailings might be expected at OB30 around 2027.

There is evidence to suggest that sulphate enrichment of groundwater at the primary bores OB 7a (SE tailings dam) and OB19a (SW) is starting to take place. As yet there is no indication that magnesium is affected. The latter is in the proximity of OB4a which is classed as a tertiary bore. The implication of groundwater movement from the SW of the tailings dam is that over time the Gulungul Creek catchment might be impacted upon. It would therefore be important to quantify solute fluxes in this direction and the degree of connection between the fractured and alluvial aquifers in this area.

A number of tertiary bores showed Mn enrichment of groundwater but only in a few was the data sufficiently extensive to allow modelling to be applied. In all cases, however, the gradient of the slope (see OB4a and OB15 in Table 5) or breakthrough time (OB13a in Table 6) indicated that Mn had a greater retardation factor than Mg which is in keeping with surface sorption site preference for the former.

In turn, the behaviour of U, given a slightly acid–circumneutral groundwater pH (see Tables 8–12, is expected to be less conservative than Mn. There is no evidence to suggest from any tertiary bores which have shown sulphate breakthrough that uranium concentrations have increased to any marked extent although upward trends are shown (typified by OB 16 in Fig 12). However, in the case of OB13a from 1992/93 onwards, anomalous high values in the order of 200–>1000 µg/L have been observed which have since declined over the last two years. These unusually high concentrations may be linked to the dumping pattern of rock types to the north of the tailings dam wall. In recent years, a problem with enhanced leaching of U from very low grade waste rock (Material 2) in the area has been noted. However, the first incidences of unusually high U concentrations in OB13a groundwater predates this.

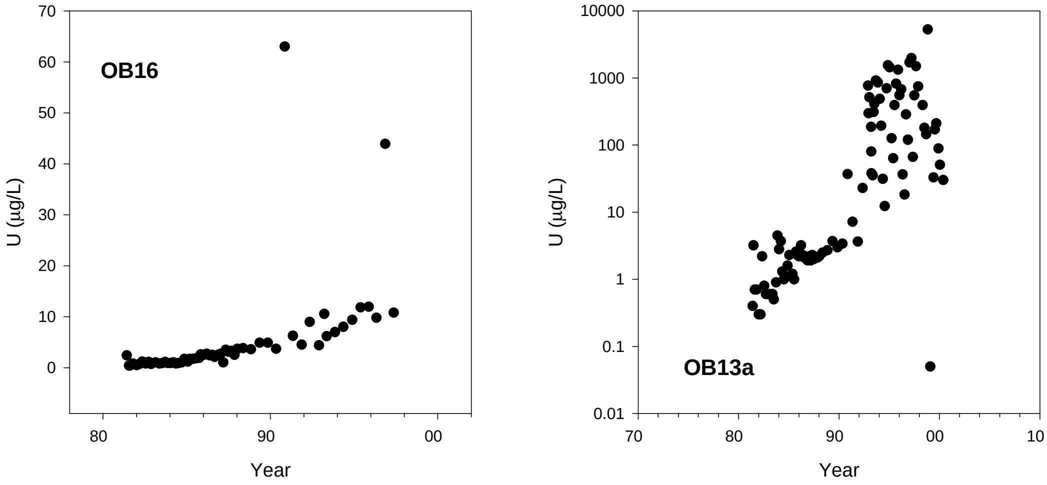

Fig 12 Trends in dissolved U concentration at OB 16 and 13a

Downgradient of OB13a, dissolved U at RN23552 has also increased although the degree of change is not shown as marked in OB44 which is in close proximity (Fig 13). Each bore is located near to SED2B from which leachate emanating the northern rock stockpile is known to have reached during the 1998/99 wet season and to a lesser extent in 1999/2000. RN23552 is a far shallower bore (slotted depth 2.9m; depth 4.6 m) compared to OB44 (Table 4) and has obviously been contaminated to a greater extent.

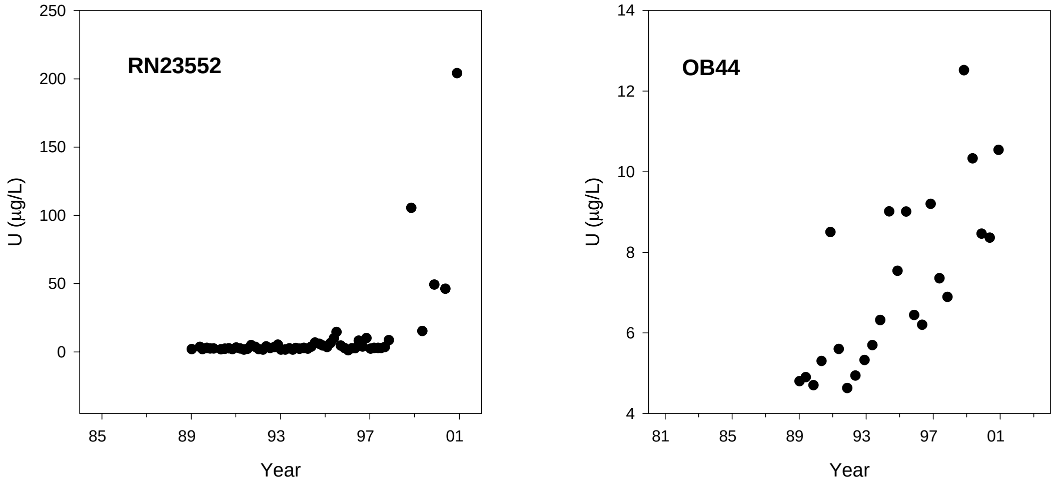

Fig 13 Trends in dissolved U concentration at RN23552 and OB44

The chemical behaviour of ^{226}Ra is such that the combination of selective sorption to oxyhydroxides and clays and the low solubility of $RaSO_4$[2] leads to its having a high retardation factor when considering its potential movement from tailings to groundwater. In a number of tertiary bores, ^{226}Ra has increased slightly over 20 years from background (typically <20 mBq/L) to around 200 mBq/L. This enhanced activity, however, is still well below the equivalent equilibrium concentration of Ra^{2+} (by 3–4 orders of magnitude) which would be obtained from a $RaSO_4$ saturated solution. Paradoxically, it is the formation[3] of the complex ion $RaSO_4^0$ which probably contributes most to the migration of Ra in solution. At a sufficiently high alkalinity, the formation[4] of $RaCO_3^0$ will also abet the movement of ^{226}Ra although at Ranger this is likely to be limited to dolomitic limestone zones.

Conclusions

- Estimated breakthrough times, using sulphate as a conservative tracer, has revealed maximum rates of solute movement of 2–8*10^{-7} ms^{-1} in groundwater of the weathered schist rock aquifer, in the vicinity of the tailings dam, which is in good agreement with previous estimates
- There is evidence to suggest that breakthrough of sulphate is starting to occur at OB19a (to the SW of the tailings dam) which will augment the migration of $MgSO_4$ which is already taking place in a similar direction nearby (at OB4a). There is the need to assess the implications of this movement to the possible impact on water quality in the Gulungul Ck catchment.

---

[2] $K_{sp} = 3.66*10^{-11}$

[3] log K = 2.43

[4] log K = 2.48

- Results from OB30 suggest that conservative salts in tailings may breakthrough from Pit #1 around 2027. The implications of this to the Corridor Ck catchment should be investigated.
- Abnormally high concentrations of dissolved U in recent years at RN23552, a shallow bore in the RP1 catchment, strongly suggests the influence of leachate from the northern waste rock stocpile.

References

Duerden P, Lever DA, Sverjensky DA & Townley LR 1992. *Summary of findings.*Final Report Vol 1, Alligator Rivers Analogue Project, Australian Nuclear and Technology Organisation.

Coffey & Hollingsworth Pty Ltd (1976). Ranger enquiry-Seepage losses from the tailings dam. Ranger Document 2129-14 (Coffey 7881B/6).

Salama R & Foley G 1997. Ranger Regional Hydrogeology Conceptual Model. ERA Environmental Services Pty Ltd.

Table 8 Summary of the composition of primary bores 1A, 7A, 17A, 19A and 20

Bore	Variable	n	$\bar{x}$	σ	median	min	max	Q_1	Q_3
1A	pH	80	6.51	0.17	6.50	6.15	7.10	6.40	6.60
	EC (µS/cm)	122	199	22	200	128	251	184	217
	Mg (mg/L)	113	7.47	1.40	7.40	2.30	11.00	6.50	8.25
	Mn (µg/L)	68	1197.3	257.3	1199.0	520.0	1800.0	1046.0	1375.0
	^{226}Ra (mBq/L)	35	60.0	40.9	50.0	29.0	210.0	38.0	65.0
	SO_4	113	0.25	0.85	0.10	0.02	9.00	0.05	0.21
	U (µg/L)	52	0.86	2.01	0.32	0.01	12.52	0.06	0.72
7A	pH	64	6.92	0.32	6.90	5.75	7.74	6.80	7.06
	EC (µS/cm)	104	384	36	388	166	471	377	403
	Mg (mg/L)	95	26.6	4.43	27.0	6.30	34.0	25.3	29.2
	Mn (µg/L)	52	54.2	66.7	26.0	5.08	383.4	14.0	85.1
	^{226}Ra (mBq/L)	17	157.5	64.7	150.0	82.1	291.6	98.9	210.0
	SO_4	93	2.32	2.95	1.10	0.05	13.29	0.65	2.40
	U (µg/L)	32	9.78	19.5	4.94	1.71	112.4	2.96	7.96
17A	pH	70	6.95	0.28	6.92	5.95	7.66	6.75	7.10
	EC (µS/cm)	113	261	43	255	177	488	244	266
	Mg (mg/L)	104	9.27	2.08	8.82	4.60	20.00	8.28	9.39
	Mn (µg/L)	59	185.8	351.0	31.2	0.5	1600.0	13.0	130.0
	^{226}Ra (mBq/L)	28	119.4	67.3	96.0	34.0	289.9	75.8	174.1
	SO_4	105	3.59	3.96	2.55	0.72	33.00	2.33	3.09
	U (µg/L)	43	6.86	7.92	3.03	1.28	39.0	2.42	8.10
19A	pH	67	6.90	0.21	6.84	6.60	7.50	6.77	7.00
	EC (µS/cm)	110	356	16	355	310	427	348	362
	Mg (mg/L)	101	19.66	1.92	19.64	10.00	24.59	19.00	20.9
	Mn (µg/L)	58	254.0	62.6	250.3	130.0	575.4	220.0	272.1
	^{226}Ra (mBq/L)	28	243.1	142.1	220.7	140.0	930.0	190.0	242.7
	SO_4	101	2.52	5.12	1.72	0.05	23.3	0.05	1.71
	U (µg/L)	40	2.92	9.89	1.10	0.05	62.13	0.51	1.63
20	pH	55	6.89	0.31	6.83	6.40	7.70	6.70	7.04
	EC (µS/cm)	98	231	30	221	191	338	213	244
	Mg (mg/L)	83	15.15	1.16	15.14	11.34	18.00	14.48	16.00
	Mn (µg/L)	39	31.4	15.6	29.0	3.0	78.0	22.0	39.0
	^{226}Ra (mBq/L)	31	26.3	17.5	28.0	1.0	69.2	8.9	40.0
	SO_4	91	0.77	0.96	0.53	0.05	8.40	0.39	0.91
	U (µg/L)	44	0.78	0.55	0.60	0.20	2.33	0.45	0.89

Table 9 Summary of the composition of primary bores 24, 30, 41, 42A and 23551

Bore	Variable	n	$\overline{x}$	σ	median	min	max	Q_1	Q_3
24	pH	76	6.81	0.37	6.70	5.89	8.20	6.60	7.00
	EC (µS/cm)	119	335	38	339	233	529	310	349
	Mg (mg/L)	110	22.35	3.20	23.00	8.68	29.74	21.00	24.05
	Mn (µg/L)	64	91.4	186.2	37.5	2.1	1420.3	14.9	96.5
	^{226}Ra (mBq/L)	36	111.5	139.1	61.0	1.0	770.0	30.4	167.5
	SO_4	108	1.58	2.19	0.70	0.05	18.55	0.43	1.80
	U (µg/L)	47	5.37	8.79	3.76	0.81	59.00	1.28	5.70
30	pH	70	7.67	0.26	7.70	6.88	8.14	7.52	7.89
	EC (µS/cm)	109	303	67	272	222	442	244	377
	Mg (mg/L)	85	34.56	8.48	30.91	22.00	55.62	29.00	37.42
	Mn (µg/L)	46	4.0	5.6	2.3	0.5	30.6	0.5	4.4
	^{226}Ra (mBq/L)	35	10.98	16.7	1.0	1.0	80.4	1.0	18.0
	SO_4	91	4.10	5.89	0.75	0.05	24.22	0.40	6.27
	U (µg/L)	53	10.01	8.44	5.10	1.70	32.79	4.10	15.66
41	pH	37	6.73	0.28	6.64	6.27	7.47	6.57	6.91
	EC (µS/cm)	76	178	13	177	132	202	172	186
	Mg (mg/L)	68	12.2	1.06	12.4	8.66	15.00	11.7	12.9
	Mn (µg/L)	27	160.1	62.1	168.7	42.5	268.6	117.2	210.0
	^{226}Ra (mBq/L)	18	40.85	41.4	23.8	4.0	184.2	19.0	50.3
	SO_4	68	7.09	54.52	0.39	0.05	450	0.20	0.59
	U (µg/L)	30	0.39	0.32	0.32	0.05	1.52	0.20	0.44
42A	pH	31	6.58	0.27	6.50	6.22	7.48	6.40	6.67
	EC (µS/cm)	58	374	48	383	168	432	351	412
	Mg (mg/L)	50	34.59	4.75	35.00	17.41	46.9	32.83	37.59
	Mn (µg/L)	21	213.9	402.0	105.7	12.1	1921.5	39.4	227.0
	^{226}Ra (mBq/L)	12	92.7	56.5	60.9	48.0	184.8	55.2	161.4
	SO_4	50	1.27	2.19	0.87	0.05	15.84	0.48	1.47
	U (µg/L)	24	2.23	1.34	1.82	1.01	7.59	1.52	2.52
23551	pH	68	6.09	0.31	6.10	5.25	6.98	5.88	6.26
	EC (µS/cm)	75	134	46	136	43	305	128	145
	Mg (mg/L)	66	8.27	4.40	8.34	0.94	23.90	6.96	9.42
	Mn (µg/L)	58	10.7	9.3	7.8	1.8	56.0	6.3	12.0
	^{226}Ra (mBq/L)	45	15.2	14.0	11.0	3.8	79.0	9.0	15.7
	SO_4	66	5.72	17.51	0.68	0.05	87.71	0.40	1.50
	U (µg/L)	62	0.76	0.90	0.53	0.05	5.39	0.30	0.84

Table 10 Summary of the composition of secondary bores 21A, 23, 28 and 43

Bore	Variable	n	$\bar{x}$	σ	median	min	max	Q_1	Q_3
21A	pH	52	7.50	0.29	7.50	6.71	8.30	7.38	7.61
	EC (µS/cm)	94	301	21	300	211	368	293	310
	Mg (mg/L)	80	16.52	2.05	16.90	3.16	21.00	15.94	17.18
	Mn (µg/L)	36	180.1	65.9	169.1	81.0	414.1	134.8	201.4
	^{226}Ra (mBq/L)	29	155.4	46.5	160.0	19.0	230.0	123.6	191.1
	SO_4	56	0.36	0.35	0.30	0.05	1.70	0.05	0.47
	U (µg/L)	40	2.22	2.69	1.89	0.23	16.68	0.73	2.40
23	pH	76	7.33	0.28	7.32	5.84	8.00	7.20	7.42
	EC (µS/cm)	119	393	12	388	361	444	387	399
	Mg (mg/L)	109	11.10	1.52	11.09	7.60	14.00	10.00	12.00
	Mn (µg/L)	65	205.1	129.5	186.3	91.0	1100.0	150.0	226.7
	^{226}Ra (mBq/L)	35	247.8	110.3	230.0	90.4	610.0	170.0	290.0
	SO_4	74	0.51	0.45	0.50	0.05	3.58	0.30	0.59
	U (µg/L)	52	4.59	12.95	1.85	0.10	93.68	1.00	3.56
28	pH	60	7.35	0.21	7.32	6.90	7.90	7.20	7.48
	EC (µS/cm)	102	335	74	328	288	1065	322	333
	Mg (mg/L)	85	15.94	1.60	16.00	8.60	20.00	15.58	16.71
	Mn (µg/L)	43	115.6	65.8	109.0	13.3	230.0	63.2	170.0
	^{226}Ra (mBq/L)	35	47.39	30.9	37.0	16.4	130.0	26.9	65.0
	SO_4	58	0.37	0.34	0.30	0.05	2.28	0.10	0.46
	U (µg/L)	47	1.10	1.15	0.70	0.21	5.19	0.46	1.20
43	pH	19	6.41	0.35	6.32	5.93	7.28	6.20	6.65
	EC (µS/cm)	19	139	4	139	133	147	135	144
	Mg (mg/L)	20	7.29	0.44	7.22	6.63	8.06	6.98	7.73
	Mn (µg/L)	25	44.7	77.0	19.0	0.5	360.0	8.2	46.5
	^{226}Ra (mBq/L)	17	29.7	15.6	27.0	9.89	60.0	15.8	41.0
	SO_4	19	2.10	2.50	1.13	0.04	7.23	0.16	4.46
	U (µg/L)	25	2.11	0.38	1.98	1.50	3.10	1.84	2.39

Table 11 Summary of the composition of tertiary bores 2A, 4A, 6A, 10A and 13A

Bore	Variable	n	$\bar{x}$	σ	median	min	max	Q_1	Q_3
2A	pH	54	6.18	0.20	6.10	5.79	6.62	6.04	6.26
	EC (µS/cm)	90	176	40	157	122	321	155	180
	Mg (mg/L)	85	9.75	2.76	9.30	1.40	22.20	8.70	10.47
	Mn (µg/L)	49	9.6	11.5	5.6	0.5	61.9	3.0	11.9
	^{226}Ra (mBq/L)	19	43.0	29.8	36.2	10.2	117.8	21.6	49.4
	SO_4	85	8.08	16.64	0.78	0.20	91.29	0.50	8.70
	U (µg/L)	31	1.52	0.90	1.30	0.10	5.69	1.20	1.73
4A	pH	69	6.43	0.17	6.40	6.10	7.00	6.30	6.50
	EC (µS/cm)	105	656	758	255	155	3555	233	788
	Mg (mg/L)	99	41.68	68.45	13.00	2.00	391.61	12.00	45.50
	Mn (µg/L)	68	997.0	1584.0	480.0	53.0	8036.0	275.0	685.0
	^{226}Ra (mBq/L)	36	136.2	150.5	105.0	60.0	960.0	82.0	123.4
	SO_4	100	215.9	488.5	3.0	0.10	2695.5	0.30	215.7
	U (µg/L)	49	2.39	4.68	1.30	0.05	31.90	0.41	2.50
6A	pH	64	6.78	0.45	6.66	6.10	8.30	6.46	7.00
	EC (µS/cm)	64	616	368	455	266	1631	366	751
	Mg (mg/L)	60	43.96	31.51	29.50	18.00	164.1	25.00	50.66
	Mn (µg/L)	61	90.1	215.8	22.0	2.0	1528.7	9.10	75.2
	^{226}Ra (mBq/L)	48	397.8	224.5	330.0	190.0	1500.0	289.8	422.5
	SO_4	59	131.9	256.7	28.0	1.6	1291.9	14.0	137.9
	U (µg/L)	59	31.65	26.11	22.95	9.60	145.71	17.00	32.71
10A	pH	82	6.66	0.32	6.60	5.78	8.20	6.47	6.85
	EC (µS/cm)	118	626	485	405	166	3139	277	875
	Mg (mg/L)	110	62.60	54.24	36.00	6.70	242.0	28.00	84.0
	Mn (µg/L)	73	41.0	48.8	21.0	3.0	290.0	7.9	61.6
	^{226}Ra (mBq/L)	37	170.2	210.9	80.0	43.0	776.3	61.1	140.1
	SO_4	110	177.7	326.2	37.0	0.1	2365.3	1.7	238.0
	U (µg/L)	52	41.2	95.0	12.0	1.8	504.0	9.8	34.0
13A	pH	99	6.39	0.32	6.36	5.91	8.70	6.20	6.50
	EC (µS/cm)	100	1699	1147	1785	177	3380	477	2888
	Mg (mg/L)	95	193.3	159.6	140.0	0.1	454.9	36.0	372.8
	Mn (µg/L)	95	341.4	275.7	240.0	14.0	956.8	110.0	606.8
	^{226}Ra (mBq/L)	66	86.5	82.9	58.3	19.0	477.1	42.0	99.8
	SO_4	94	893.6	833.8	670.0	2.2	3564.1	72.2	1624.1
	U (µg/L)	95	228.5	428.3	7.2	0.3	1980.1	2.1	249.2

Table 12 Summary of the composition of tertiary bores 29, 44, 23552 and 79/2

Bore	Variable	n	$\bar{x}$	σ	median	min	max	Q_1	Q_3
29	pH	65	7.54	0.15	7.50	7.26	7.80	7.40	7.7
	EC (µS/cm)	68	522	175	432	366	915	410	624
	Mg (mg/L)	60	60.40	20.78	53.00	34.00	123.5	48.25	59.5
	Mn (µg/L)	61	14.3	21.7	4.0	0.5	93.5	2.0	17.6
	^{226}Ra (mBq/L)	34	48.0	48.4	26.7	10.0	230.0	20.0	64.2
	SO_4	62	59.9	109.9	6.4	0.2	442.7	1.0	50.0
	U (µg/L)	59	12.69	4.74	13.00	2.94	31.00	10.15	15.00
44	pH	28	6.40	0.28	6.34	6.10	7.42	6.22	6.42
	EC (µS/cm)	62	1096	451	1041	466	2244	699	1404
	Mg (mg/L)	57	99.31	51.26	86.50	0.05	274.0	55.55	134.88
	Mn (µg/L)	23	41.1	48.7	24.1	0.5	190.6	10.5	53.5
	^{226}Ra (mBq/L)	19	91.5	63.7	71.0	28.0	252.3	43.3	130.0
	SO_4	57	434.1	444.7	347.7	64.0	3084	182.5	569.3
	U (µg/L)	24	7.19	2.17	7.06	4.63	12.52	5.31	8.88
23552	pH	63	6.10	0.43	6.01	5.47	9.01	5.90	6.12
	EC (µS/cm)	63	789	461	669	70	1843	388	1148
	Mg (mg/L)	58	73.50	55.8	55.53	3.50	260.00	29.25	103.37
	Mn (µg/L)	57	15.22	20.2	9.7	0.50	127.3	5.1	16.6
	^{226}Ra (mBq/L)	46	80.8	39.7	75.5	1.00	162.7	47.2	113.4
	SO_4	57	285.0	262.2	199.6	12.7	1127.7	86.4	419.8
	U (µg/L)	57	10.81	30.45	2.90	1.27	204.01	2.36	5.14
79/2	pH	87	8.02	0.24	8.00	7.20	8.70	7.90	8.20
	EC (µS/cm)	99	554	210	466	322	1103	444	510
	Mg (mg/L)	80	70.84	31.61	61.00	0.05	156.90	57.25	68.75
	Mn (µg/L)	81	78.6	91.3	65.0	0.5	660.0	29.2	96.0
	^{226}Ra (mBq/L)	37	52.8	54.5	33.8	3.0	239.2	12.4	65.5
	SO_4	91	93.8	144.0	38.0	0.1	832.0	30.0	63.0
	U (µg/L)	79	7.23	5.77	7.30	0.40	23.63	1.30	12.00